Elucidation of the anaerobic pathway for the corrin component of cobalamin (vitamin B_{12})

Simon J. Moore[a], Andrew D. Lawrence[a], Rebekka Biedendieck[a,b], Evelyne Deery[a], Stefanie Frank[a], Mark J. Howard[a], Stephen E. J. Rigby[c,1], and Martin J. Warren[a,1]

[a]School of Biosciences, University of Kent, Kent CT2 7NJ, United Kingdom; [b]Institute of Microbiology, Technische Universität Braunschweig, 38106 Braunschweig, Germany; and [c]Manchester Institute of Biotechnology, Faculty of Life Sciences, University of Manchester, Manchester M1 7DN, United Kingdom

Edited by Jerrold Meinwald, Cornell University, Ithaca, NY, and approved July 17, 2013 (received for review May 2, 2013)

It has been known for the past 20 years that two pathways exist in nature for the de novo biosynthesis of the coenzyme form of vitamin B_{12}, adenosylcobalamin, representing aerobic and anaerobic routes. In contrast to the aerobic pathway, the anaerobic route has remained enigmatic because many of its intermediates have proven technically challenging to isolate, because of their inherent instability. However, by studying the anaerobic cobalamin biosynthetic pathway in *Bacillus megaterium* and using homologously overproduced enzymes, it has been possible to isolate all of the intermediates between uroporphyrinogen III and cobyrinic acid. Consequently, it has been possible to detail the activities of purified cobinamide biosynthesis (Cbi) proteins CbiF, CbiG, CbiD, CbiJ, CbiET, and CbiC, as well as show the direct in vitro conversion of 5-aminolevulinic acid into cobyrinic acid using a mixture of 14 purified enzymes. This approach has resulted in the isolation of the long sought intermediates, cobalt-precorrin-6A and -6B and cobalt-precorrin-8. EPR, in particular, has proven an effective technique in following these transformations with the cobalt(II) paramagnetic electron in the d_{yz} orbital, rather than the typical d_z2. This result has allowed us to speculate that the metal ion plays an unexpected role in assisting the interconversion of pathway intermediates. By determining a function for all of the pathway enzymes, we complete the tool set for cobalamin biosynthesis and pave the way for not only enhancing cobalamin production, but also design of cobalamin derivatives through their combinatorial use and modification.

cobalt | NMR | precorrin | tetrapyrrole | metabolism

Ever since the pioneering work of Dorothy Hodgkin revealed the complexity of vitamin B_{12} (cyanocobalamin) (1), chemists and biochemists have endeavored to unravel the step-by-step biosynthesis of this essential cofactor and coenzyme. The two major biologically active forms of vitamin B_{12} are methylcobalamin and adenosylcobalamin, which are composed of a highly modified cobalt-containing tetrapyrrole linked to a nucleotide loop that houses an unusual base called dimethylbenzimidazole. This base acts as a lower ligand to the cobalt ion, whereas the upper cobalt ligand is provided by either the methyl or 5′-deoxyadenosyl group (Fig. 1). The cobalt-containing modified tetrapyrrole component of the vitamin is referred to as the corrin ring and differs in size from other modified tetrapyrroles, because it has undergone contraction as part of the biosynthetic process.

Research into the biosynthesis of the corrin ring has revealed the presence of two similar, although distinct, biochemical pathways, which differ on the timing of cobalt insertion and a requirement for molecular oxygen (2). The cobalt-late or aerobic pathway is the better characterized, and all of the intermediates and enzymes responsible for the de novo construction of the corrin component have now been determined (3, 4). In contrast, the cobalt-early or anaerobic pathway is poorly delineated. Many of the pathway intermediates remain hypothetical and are based on the order of events that have been determined in the aerobic pathway (4), because both pathways use a number of similar enzymes (Fig. 1) (5, 6).

Corrin ring synthesis is initiated from uroporphyrinogen III, the first macrocyclic intermediate of the tetrapyrrole pathway (7). The corrin intermediates are then defined by the number of *S*-adenosyl-L-methionine (SAM) -derived methyl groups that have been added to the framework (8). For instance, precorrin-2 is so called, because two methyl groups have been added to uroporphyrinogen III by CobA. Oxidized versions of these intermediates are called factors, where factor II is the oxidized version of precorrin-2. In *Bacillus megaterium*, which operates an anaerobic cobalamin biosynthetic pathway (6), corrin ring synthesis progresses by insertion of cobalt into factor II (9–11). This cobalt complex is further methylated at C-20 to give cobalt-factor III by CbiL, a member of the canonical methyltransferases associated with cobalamin synthesis (12). The next reaction is facilitated by $CbiH_{60}$ to give cobalt-precorrin-4 in a reaction that requires reducing equivalents to ensure a high yield of product (13).

Cobalt-precorrin-4 has previously been shown to be a pathway intermediate, because its incubation in a cell-free lysate of *Propionibacterium shermanii* resulted in its transformation into cobyrinic acid, albeit in a very low yield (~1%) (14). It has also been shown that cobalt-precorrin-4 can be converted into cobalt-precorrin-5A by *Escherichia coli* extracts that contain overproduced *Salmonella enterica* CbiF in the presence of SAM in a yield of ~5–10% (15). Similarly, cobalt-precorrin-4 can be transformed into cobalt-precorrin-5B by incubation with cell lysates containing CbiF and CbiG, indicating that CbiG catalyses the opening of the δ-lactone ring and the subsequent deacylation (15) to release the C2 fragment as acetaldehyde (16). However, the poor conversion rates of these reactions have prevented a detailed study of the mechanisms underpinning these transformations, and all of the intermediates have been characterized only as their derivatized methylester form rather than as free acids.

The lack of any isolated intermediates between cobalt-precorrin-5B and cobyrinic acid means that a black box exists for the latter portion of the anaerobic corrin synthesis pathway (Fig. 1). From cobalt-precorrin-5B, the C-1 position is the next expected methylation site (8). In the aerobic pathway, this step is catalyzed by a class III SAM-dependent methyltransferase, CobF. However, no equivalent enzyme is found in the anaerobic pathway. Evidence that CbiD catalyzes the C-1 methylation has been implied from indirect genetic engineering studies on whole cells (17), although this result has not been reproduced with purified enzymes; also, the expected product cobalt-precorrin-6A has not been isolated. A structure (*Archaeoglobus fulgidus*; Protein Data Bank ID code 1SR8) of CbiD was released, but it shares no similarity to any characterized enzyme, and the protein does not

Author contributions: S.J.M., A.D.L., R.B., E.D., S.F., M.J.H., S.E.J.R., and M.J.W. designed research; S.J.M., A.D.L., R.B., E.D., S.F., and S.E.J.R. performed research; S.J.M. and R.B. contributed new reagents/analytic tools; S.J.M., A.D.L., M.J.H., S.E.J.R., and M.J.W. analyzed data; and S.J.M., S.E.J.R., and M.J.W. wrote the paper.

The authors declare no conflict of interest.

This article is a PNAS Direct Submission.

See Commentary on page 14823.

[1]To whom correspondence may be addressed. E-mail: stephen.rigby@manchester.ac.uk or m.j.warren@kent.ac.uk.

This article contains supporting information online at www.pnas.org/lookup/suppl/doi:10.1073/pnas.1308098110/-/DCSupplemental.

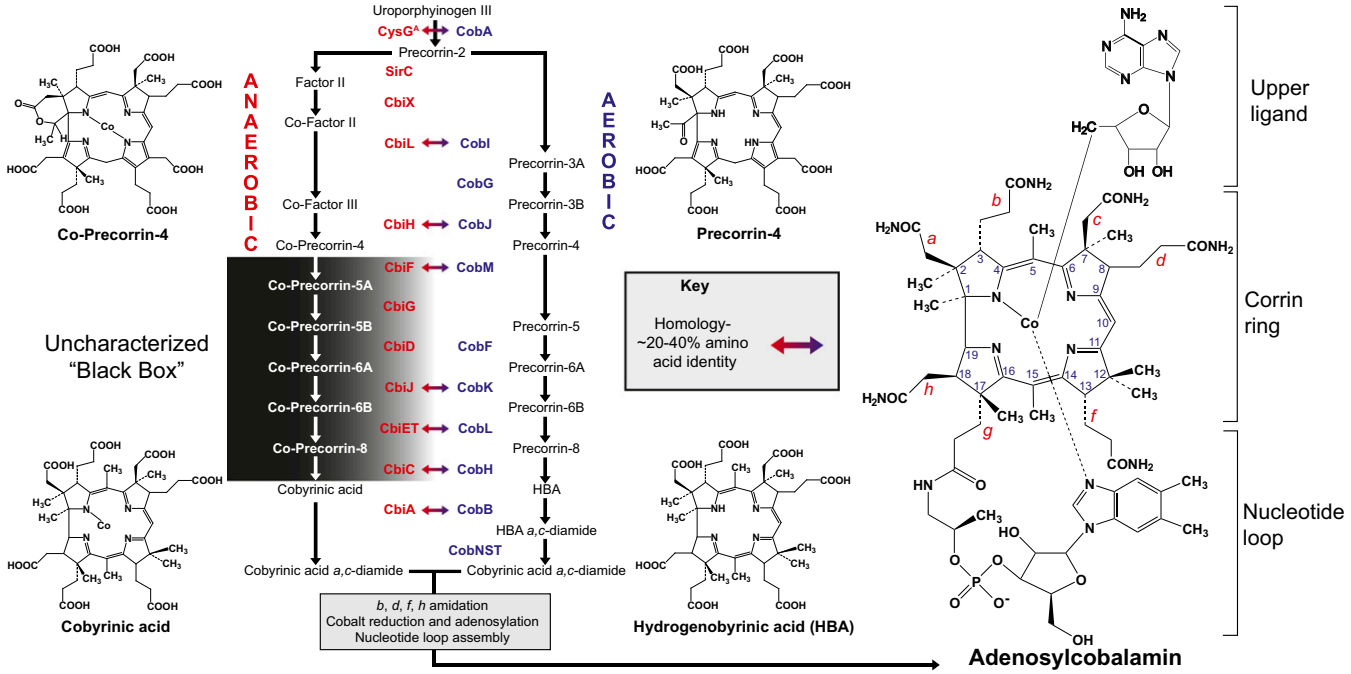

Fig. 1. Summary of the aerobic and anaerobic cobalamin biosynthetic pathways from precorrin-2 to cobyrinic acid *a,c*-diamide. The fully characterized aerobic pathway (blue) is compared with the anaerobic pathway (red), and many of the steps are predicted from sequence homology to the aerobic pathway (30–32). These unknown steps are referred to as the black box.

contain a Rossman fold, which is considered an essential structural feature for SAM binding. For the rest of the pathway, the intermediates and reactions have yet to be isolated. Indeed, the enzymes CbiJ, CbiE, CbiT, and CbiC share reasonable homology (~20–40% amino acid identity) to enzymes from the aerobic pathway that have been characterized and shown to convert precorrin-6 to hydrogenobyrinic acid (3, 4). A summary of the aerobic and anaerobic pathways is shown in Fig. 1.

In this report, we describe the complete elucidation of the elusive anaerobic vitamin B_{12} pathway, one of the last uncompleted chapters in tetrapyrrole biosynthesis. With respect to the chemical logic of this biosynthesis, the exposition of the anaerobic pathway has provided insights into the chemistry and evolution of this remarkable process, which represents one of the longest biosynthetic pathways found in nature.

Results

Homologous Production of Cobalamin Enzymes in *B. megaterium*. The cobalamin biosynthetic enzymes were produced homologously in *B. megaterium* by cloning the relevant genes (Table S1 shows plasmids and primers) with a fusion to a His_6-tag within plasmid pC-His1622 or pN-His-TEV1622 (18). These genes included (in order of predicted enzymatic reactions) *cbiF*, *cbiG*, *cbiD*, *cbiJ*, *cbiET*, and *cbiC*. Recombinant strains were obtained by protoplast transformation of *B. megaterium* DSM319 with a modified minimal media method (*SI Text*). After growth and overproduction by xylose induction, each protein was individually purified to homogeneity (Fig. S1 and Table S2). This approach allowed significant quantities of soluble and relatively pure protein to be isolated. Furthermore, all these enzymes were stable in the standard buffers described (20 mM Tris·HCl, Hepes, pH 7–8, 100 mM NaCl), with the exception of CbiF and $CbiH_{60}$ (13), both of which required a high salt concentration (400 mM) to maintain solubility at 5–10 mg mL^{-1}. The aggregation state of the various proteins was estimated by size exclusion chromatography (Table S2).

Synthesis of Cobalt-Precorrin-5A. Cobalt-precorrin-5A and -5B had not been characterized in their free acid forms, because the yields of these intermediates were very low when previously detected (5–10%). The activity of purified *B. megaterium* CbiF with cobalt-precorrin-4 was, therefore, monitored to try and improve the conversion into cobalt-precorrin-5A. Incubation of CbiF with SAM and cobalt-precorrin-4 leads to gradual changes in the color of the substrate, with a change from pale red to red-orange. Nonetheless, despite increasing the enzyme concentration, conversion into this species was not improved. Cobalt-precorrin-4 can be separated from this species on a DEAE–Sephadex column. The UV-visible spectrum of this product has a broad absorbance peak at 340 nm and a minor peak at 440 nm (Fig. 2). Liquid chomatography (LC)-MS showed that the substrate cobalt-precorrin-4 is detected at *m/z* 950, whereas the product of the CbiF reaction is detected with an *m/z* 964 (Fig. S2). This result shows an increase of 14 Da consistent with the addition of a methyl group and a molecular formula ($C_{45}H_{53}CoN_4O_{16}$) in agreement with cobalt-precorrin-5A.

Synthesis of Cobalt-Precorrin-5B. Previously, CbiG had been shown to open the δ-lactone on ring A and release the methylated C-20 carbon as a C2 fragment in the form of acetaldehyde (16), generating the intermediate cobalt-precorrin-5B (15). This reaction is a prerequisite to the C-1 methylation step (8). Using cobalt-precorrin-5A, the activity of CbiG was recorded by the following changes in the UV-Vis spectrum of the substrate. The visual appearance changed from orange-red to a bright orange-colored solution. During the incubation, the Soret peak at 337 nm shifts to give a clear peak at 355 nm, with a slight shoulder at 388 nm (Fig. 2). In addition, the minor absorbance peak at 440 nm is replaced with double peaks at 469 and 500 nm. However, this intermediate is extremely sensitive to oxygen and when exposed to air, undergoes an instantaneous change to a pale brown pigment. Because of this rapid oxidation, LC-MS could not be used to determine the true mass of this intermediate, with only degraded fragments at *m/z* 920 (Fig. S2) and *m/z* 904 detected. The expected mass for cobalt-precorrin-5B is 937 Da. However, if kept under anaerobic conditions (<2 ppm O_2), the orange-colored product of the CbiG reaction, cobalt-precorrin-5B, remains stable for several months.

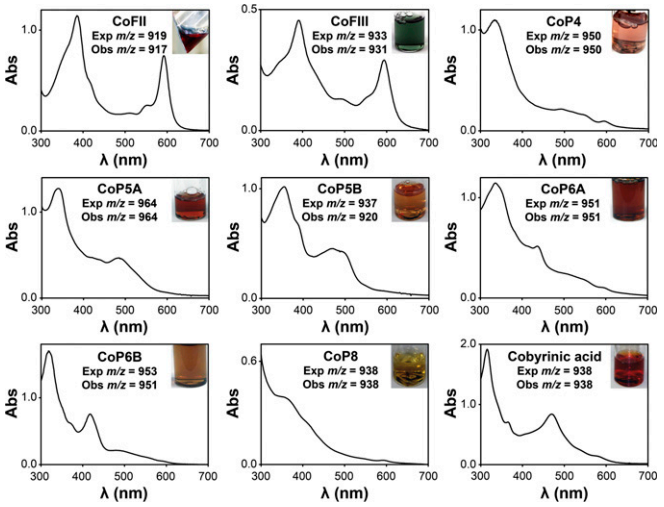

Fig. 2. Intermediates of the anaerobic biosynthesis of cobalamin. Panels show the UV-Vis spectrum, MS, and visual appearance of each intermediate between cobalt-factor II and cobyrinic acid. Intermediates are Cobalt-Precorrin (CoP) and Cobalt-Factor (CoF). MS data are shown in Fig. S2. Exp, expected; obs, observed.

Enhanced Synthesis of Cobalt-Precorrin-5B from Cobalt-Factor III. The activity of CbiF was found to be very poor on direct incubation with cobalt-precorrin-4 and SAM, with yields typically in the 10–20% range. Interestingly, higher yields could be achieved by combining the enzymes $CbiH_{60}$, CbiF, and CbiG with the cofactors SAM and dithionite, and the substrate cobalt-factor III in an enzyme-mixture incubation (*SI Text* and Fig. S3*A*). Typically, this approach achieves a repeatable >80% transformation of cobalt-factor III into cobalt-precorrin-5B.

Synthesis of Cobalt-Precorrin-6A. Based on pulse-labeling experiments (8), it was known that the C-1 methylation step is the next reaction in the pathway, with CbiD most likely to catalyze this methylation (17). To show this activity conclusively, *B. megaterium* CbiD was incubated with cobalt-precorrin-5B and SAM, which resulted in the UV-Vis spectrum of the incubation becoming blue-shifted during the reaction (Fig. 2 and Fig. S3*B*). The UV-Vis spectral changes are accompanied with a subtle color change from orange to a red-bronze pigmentation. This intermediate could be detected by LC-MS (Fig. S4) with a dominate mass at *m*/*z* 951 (Fig. S2), which represents an increase of 14 Da. It is consistent with the addition of a methyl group, and it is in agreement with the predicted molecular formula ($C_{44}H_{50}CoN_4O_{16}$) for cobalt-precorrin-6A.

EPR has previously been used for the characterization of the early steps of the anaerobic B_{12} pathway, including cobalt chelation into sirohydrochlorin by $CbiX^L$ (9), C-20 methylation by CbiL (12, 19), and ring contraction reaction by $CbiH_{60}$ (13). For EPR, we shall now refer to each intermediate as cobalt(II)-precorrin-*n*, because all the pathway intermediates that we have analyzed are in the detectable paramagnetic cobalt(II) form. Thus, we do not lose or gain cobalt(II) signal in any of the reactions, indicating that cobalt(II) is not oxidized or reduced under the conditions tested.

The previous EPR studies mentioned above presented spectra of low-spin cobalt(II) ions having one unpaired electron in the d_z2 orbital. Such spectra exhibit axial or nearly axial anisotropy, having $g_{||} \sim 2$ and $g_{\perp} = 2.2$–3.0, and a relatively large anisotropic cobalt hyperfine interaction, giving $A_{||}^{Co} \sim 100$ G. Most low-spin cobalt(II) compounds, including derivatives of coenzyme B_{12}, give rise to EPR spectra of this class. Unexpectedly, cobalt(II)-precorrin-5B and -6A do not match this class of EPR spectra and instead, most closely resemble EPR spectra of a nonbiological complex in an N_4 macrocycle (20–23). Unusually, the cobalt(II) unpaired electron resides in the ground state d_{yz} orbital (Fig. S5), with electron donation from two nitrogen ligands. In contrast, for most B_{12} pathway intermediates, the four nitrogen atoms liganded to the cobalt(II) share one negative charge. The EPR spectra of these d_{yz} compounds are normally described as rhombic and characterized by three *g* values attributed as g_x, g_z, and g_y (although the difference between g_z and g_y may be small), with the *z* direction being perpendicular to the ligand plane, whereas *x* and *y* are mutually orthogonal within that plane. Although g_x is always the largest (lowest field) *g* value in such compounds, the order in which g_y and g_z occur depends on the compound in question; therefore, we shall simply refer to *g* tensors as g_1, g_2, and g_3 beginning at the lowest field. The theory underpinning the ground state electronic configurations of low-spin cobalt(II) compounds and the nature of the singly occupied molecular orbital have been presented (24, 25).

Cobalt(II)-precorrin-5B displays three *g* values ($g_1 = 2.72$, $g_2 = 2.06$, and $g_3 = 1.96$) and resolved hyperfine coupling at $|A_3| = 31.8$ G (Fig. 3 and Table S3). Cobalt(II)-precorrin-5A gives rise to a very similar spectrum (parameters are shown in Table S3); however, these data cannot be obtained without a contaminating

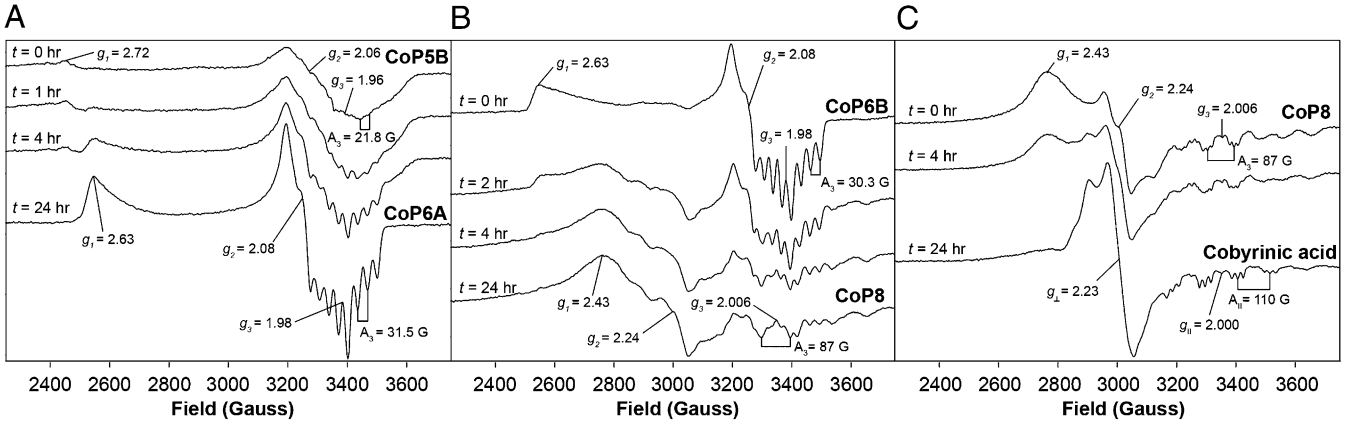

Fig. 3. EPR of some of the anaerobic pathway steps. (*A*) Reaction of 50 μM CbiD, 200 μM cobalt(II)-precorrin-5B, and 2 mM SAM incubated at 37 °C for 24 h. Samples were removed at $t = 0$, 1, 4, and 24 h. (*B*) Reaction of 20 μM CbiET, 200 μM cobalt(II)-precorrin-6B, and 2 mM SAM at 37 °C. Samples were removed at $t = 0$, 2, 4, and 24 h. (*C*) Reaction of 10 μM CbiC and 200 μM cobalt(II)-precorrin-8 incubated at 37 °C for 24 h. Samples were removed at $t = 0$, 4, and 24 h. *g* Values and coupling constants of hyperfine splittings are shown here and in Table S3. Spectra were recorded at 20 K using a microwave power of 1 mW, a modulation frequency of 100 kHz, and a modulation amplitude of 5 G. Negative control spectra are shown in Fig. S6.

cobalt(II)-precorrin-4 spectrum that must be removed computationally because of the failure of the CbiF-catalyzed methylation to reach completion (see above). Addition of SAM does not lead to changes in the EPR spectrum of cobalt(II)-precorrin-5B (Fig. S6). Furthermore, the EPR spectrum of a negative-control reaction with CbiD (no SAM) does not reveal any changes in the spectrum over a time period (Fig. S6). For the complete reaction (with SAM), gradual changes in the EPR spectra resulted over the time course (Fig. 3*A*). We attribute this change to the formation of cobalt(II)-precorrin-6A. The EPR spectrum of cobalt(II)-precorrin-6A retains similar features with $g_1 = 2.63$, $g_2 = 2.08$, $g_3 = 1.98$, and $|A_3| = 31.5$ G. Most notably, the line shape and intensity of the hyperfine splittings are enhanced. Because the d_{yz} orbital is retained after C-1 methylation by CbiD, the changes in line shape and enhanced splitting suggest a change in conjugation in the macrocycle and enhanced conformational stability. One plausible explanation is methylation at C-1 and consequent prototropic rearrangement of the double bond at C-1/C-19 to the C-19/C-18 position.

Synthesis of Cobalt-Precorrin-6B. In the aerobic pathway, CobK drives the NADPH-dependent reduction of the C-18/C-19 double bond to convert precorrin-6A into precorrin-6B. Because of sequence identity with CobK (~20–30%), it was assumed that CbiJ catalyzes the equivalent reaction by converting cobalt-precorrin-6A into cobalt-precorrin-6B. When cobalt-precorrin-6A was incubated with CbiJ and NADPH, there was no change observed in the UV-Vis spectrum of the substrate, suggesting that no reaction had taken place. However, when NADPH was replaced with NADH in the incubation, a change in the absorbance spectrum of the incubation was observed, with the peaks at 335 and 436 nm shifting to 318 and 419 nm, respectively (Fig. 2 and Fig. S3*C*). These changes were not observed in any of the controls (NADH, NADPH, or enzyme only), indicating that the reaction is dependent on the presence of CbiJ and NADH. The rate of the CbiJ-catalyzed reaction was very fast (seconds), similar to the level of activity observed with CbiG. The NADH-dependent reduction of cobalt-precorrin-6A into cobalt-precorrin-6B is expected to occur at the C-18/C-19 double bond, with a gain of two mass units. We attempted to show this change by MS but found that cobalt-precorrin-6B was unstable. Lowering the pH below 6.5 results in an instant bleaching (dark to pale red) of the color for both cobalt-precorrin-6A and cobalt-precorrin-6B. This change leads to a UV-Vis spectrum that is identical for both intermediates. Both cobalt-precorrin-6A and the expected product of the CbiJ reaction, cobalt-precorrin-6B, are detected with an identical retention time and mass at *m/z* 951 (Fig. S2). We were unable to solve the structure of the intermediate by NMR, possibly because of the presence of a number of tautomeric species (*SI Text* and Fig. S7).

Synthesis of Cobalt-Precorrin-8. In some organisms operating the anaerobic pathway, the transformation of cobalt-precorrin-6B into cobalt-precorrin-8 is mediated by two enzymes CbiE and CbiT. It is thought that CbiE is responsible for the methylation at C-5, whereas CbiT couples the decarboxylation of the ring C acetate side chain with methylation at C-15. In the aerobic pathway, these two enzymes are always found fused together in a protein called CobL, and a similar situation occurs with the anaerobic pathway in *B. megaterium* with the presence of CbiET. The activity of CbiET was initially monitored by UV-Vis spectroscopy, where the spectrum of cobalt-precorrin-6B was observed to bleach, concomitant with a color change from dark red to pale yellow (Fig. 2 and Fig. S3*D*). LC-MS showed that cobalt-precorrin-6B (*m/z* 951) is converted into major and minor products at *m/z* 938 and *m/z* 936 (Fig. S4), respectively. The UV-Vis spectrum of the major peak at *m/z* 938 matches the spectrum described above, whereas its mass is consistent for the expected product cobalt-precorrin-8 ($C_{45}H_{59}CoN_4O_{14}$).

Major changes were detected in the EPR spectra during the conversion of cobalt(II)-precorrin-6B to cobalt(II)-precorrin-8 (Fig. 3*B*). Over the time period of the reaction, the three *g* values (g_1, g_2, and g_3) of cobalt(II)-precorrin-6B are replaced by three new *g* values: $g_1 = 2.43$, $g_2 = 2.24$, and $g_3 = 2.006$. Compared with cobalt-precorrin-6B, the field range narrows between g_1 and g_3 for cobalt-precorrin-8, whereas g_2 and g_3 separate, and the cobalt hyperfine splittings increase from 30.3 to 87 G. This observation suggests a change in electronic structure, in which the unpaired electron is once again mainly in the d_z2 orbital. In addition, a superhyperfine interaction with a nitrogen (^{14}N) ligand leading to triplet formation is observed in this region, which may be caused by a contaminating N ligand, possibly from the buffer. Such a superhyperfine coupling would not be observed if the unpaired electron was located in the d_{yz} orbital.

Synthesis of Cobyrinic Acid. To complete the pathway to cobyrinic acid, the final reaction in the series is the methylmutase CbiC. In the aerobic pathway, the equivalent enzyme, CobH, oversees an unusual 1,5-sigmatropic rearrangement, where the C-11 methyl group migrates to the C-12 position, creating a quaternary carbon center. Cobalt-precorrin-8 is a pale yellow intermediate. However, on incubation with CbiC, a slow but progressive change occurs as the intermediate changes to a golden orange-colored intermediate. Incubation of 5 μM CbiC and 45 μM cobalt-precorrin-8 at 37 °C for 6 h yielded a UV-Vis spectrum that resembles a typical cobalt B_{12}-like spectrum with a Soret peak at 314 nm, whereas an additional shoulder at 465 nm is also observed (Fig. 2 and Fig. S3*E*). The mass of this intermediate was detected at *m/z* 938 (Fig. S2) and as expected, is the same as the substrate, cobalt-precorrin-8. After enzyme incubation, cob(II)yrinic acid was purified to homogeneity and then oxidized to cob(III)yrinic acid by addition of potassium cyanide. Cyanide is known to coordinate B_{12}, forming a hexacoordinated cobalt(III) ion, with cyanide bound as both upper (β) and lower (α) axial ligands. This change shifted the Soret peak to 365 nm, whereas typical B_{12}-like α- and β-bands were observed at 502, 537, and 578 nm. This intermediate eluted as two separate peaks on LC-MS, although both had identical masses at *m/z* 964. This result is consistent for monocyanocobyrinic acid. A mass for dicyanocobyrinic acid (exp *m/z* 990) was not detected; however, a standard of dicyanocobinamide is also found to elute as two peaks, both as the mono form. The two peaks on LC-MS may be caused by the pentacoordinated α- or β-cyano ligand forms.

As with the UV-Vis spectroscopy, EPR provided additional evidence for our findings, because the EPR spectrum of cobalt-precorrin-8 is converted into a new B_{12}-like spectrum, which has previously been described for base-on cobinamide (26). The product, cobyrinic acid, has *g* values at $g_\perp = 2.23$, $g_{||} = 2.000$, and $A_{||}^{Co} = 110$ G (Fig. 3*C*). These data are in agreement with published spectra of cob(II)inamides and cob(II)alamins, which like cob(II)yrinic acid, share the same UV-Vis and EPR spectra (27). The EPR spectrum of cob(II)yrinic acid seems base-on, because the superhyperfine coupling constant is 18 G. This result may be attributed to the Tris buffer or contaminating imidazole [20 G for cob(II)inamide in MeOH].

To confirm the structure of cobyrinic acid, a pure sample was synthesized directly from the starting metabolite of tetrapyrrole biosynthesis, 5-aminolevulinic acid, in a multistep mixture incubation using 14 purified enzymes HemB, HemC, HemD, CobA, SirC, CbiX, CbiL, $CbiH_{60}$, CbiF, CbiG, CbiD, CbiJ, CbiET, and CbiC. After purification to homogeneity by anion exchange and reverse-phase chromatography, 1.8 mg pure cob(II)yrinic acid were isolated [estimated at 40% yield from 5-aminolevulinic acid (ALA)]. Solid potassium cyanide was added to provide upper and lower cobalt ligands and oxidization to the cobalt(III) form. Datasets of ^{13}C-^{1}H heteronuclear single quantum coherence (Fig. S8 and Table S4), total correlation, ^{1}H-^{1}H homonuclear correlation, heteronuclear multiple bond correlation, and rotating frame Overhauser effect were collected measuring resonance of naturally abundant ^{13}C and ^{1}H. In the ^{13}C-^{1}H heteronuclear single quantum coherence spectrum, one major species (>75%) is detected representing dicyanocob(III)yrinic acid along

with two possible derivatives. Eight methyl groups at the C-1, C-2, C-5, C-7, C-12α, C-12β, C-15, and C-17 positions were detected. The C-5, C-10, and C-15 carbon positions are sp^2, which suggests the correct formation of the corrin ring system. A methylene bridge is present at C-10, whereas C-18 and C-19 are protonated. The C-1 methyl group shows nuclear Overhauser effect contacts to the C-19 proton and the ring D acetate CH_2 group, whereas the heteronuclear multiple bond correlation also reveals contacts with pyrrole ring carbons in rings A and D. The methyl group at C-1 and protons at C-18 and C-19 provide evidence for the earlier actions of CbiD and CbiJ, respectively. These findings are similar to previously published spectra of cobyrinic acid heptamethyl ester, although these data were obtained in d_6-hexane (28).

Discussion

In an attempt to elucidate completely the pathway associated with the anaerobic synthesis of the corrin ring, we took advantage of the tool box of enzymes found in *B. megaterium*. This approach proved successful, because high yields of soluble enzymes were obtained through homologous protein production. The starting point was the production of both cobalt-precorrin-5A and -5B from cobalt-precorrin-4. Although these syntheses validated the activities of CbiF and CbiG, the yields were low (10–20%) as previously noted (15). In contrast, the direct synthesis of cobalt-precorrin-5B from cobalt-factor III with an enzyme mixture incubation results in yields greater than 80%. The poor transformation from cobalt-precorrin-4 likely reflects the observation that isolated cobalt-factor IV and cobalt-precorrin-4 exist in multiple tautomeric forms, some of which may act as inhibitors. The improvement in yield of cobalt-precorrin-5B by use of an enzyme mixture suggests that the pathway enzymes may act to facilitate substrate channeling. For the next step, we have been able to show that CbiD is active as an SAM-dependent methyltransferase, because it transforms cobalt-precorrin-5B into cobalt-precorrin-6A. This result shows that CbiD is able to catalyze the reaction in isolation and does not function only as part of a multienzyme complex (17).

The EPR spectroscopic studies provide a metallocentric view of the black box stages of adenosylcobalamin biosynthesis. The results presented here show that the cobalt ion in the early metal insertion pathway is an active participant in the biosynthesis and not merely an observer. There is no evidence that the ion undergoes oxidation/reduction reactions during the course of the biosynthesis. The cobalt ion remains in the +2 oxidation state throughout, and thus, it seems that the cobalt ion does not play the role of an electron sink, except possibly transiently. However, it is clear that the orbital structure of the ion is altered in cobalt(II)-precorrin-5A/B and cobalt(II)-precorrin-6A/B relative to other intermediates in the pathway, with the singly occupied molecular orbital (SOMO) becoming the d_{yz} orbital rather than the d_z2 orbital. Such an arrangement of the *d* electrons is very unusual and has not previously been reported for compounds isolated from biological systems, only being observed in a few synthetic compounds (29). Such synthetic compounds show that the nature of the ligand is the driving force for the rearrangement, with an increase in Lewis base character favoring the d_{yz} orbital as the SOMO (29). Thus, the cobalt ion participates in the biosynthetic pathway by contributing to the stabilization of the structures of cobalt(II)-precorrin-5A/B and cobalt(II)-precorrin-6A/B that are more electron donating and show more Lewis base character. All other intermediates in the pathway contribute only one covalent bond to cobalt and therefore, exhibit less Lewis basicity and favor the d_z2 orbital as the SOMO. Therefore, the anaerobic biosynthesis of vitamin B_{12} provides an example of a metal ion with several accessible redox states playing an unexpected role in Lewis acid/base chemistry while apparently having no redox role.

One of the major differences between the aerobic and anaerobic corrin biosynthetic pathways relates to the enzymes used to methylate the C1 position. In the aerobic pathway, this reaction is mediated by CobF, which is similar to the majority of other cobalamin biosynthetic methyltransferases. CobF aids in the removal of the extruded methylated C20 position as acetic acid and then methylates the C-1 position. The anaerobic pathway instead uses two unique enzymes: CbiG and CbiD. CbiG opens the δ-lactone ring and extrudes the methylated C20 position as acetaldehyde (16), forming cobalt-precorrin-5B. This change results in a double bond between C-1 and C-19 (15). Because the cobalt(II) unpaired electron occupies a d_{yz} orbital in cobalt-precorrin-5B, the metal behaves like a Lewis-base, allowing it to aid in the activation of the C-1 position for methyl addition by electrophilic substitution. Methylation at C-1 would also result in a prototropic rearrangement of the C-1 double bond to C-19 in ring D. This double bond, consequently, has to be reduced by CbiJ, thereby providing a chemical rationale for this sequence of reactions. The dramatic changes in UV-Vis and EPR spectra during these stages are also highly indicative of double bond rearrangement (CbiD) and reduction (CbiJ). It seems that these key differences in chemistry between the early and late cobalt insertion pathways at the C-1 methylation site have crafted two separate methyltransferase enzymes (CbiD/CobF).

The full step-by-step in vitro synthesis of cobyrinic acid from ALA requires 14 enzymes, and we have shown that this transformation can be accomplished by an enzyme mixture approach. This report also provides an accurate description of the anaerobic pathway (Fig. 4) and essentially defines the activities of enzymes involved in the black box region of the biosynthesis. In a broader context, this understanding provides an important prerequisite within the area of synthetic biology if we are to use

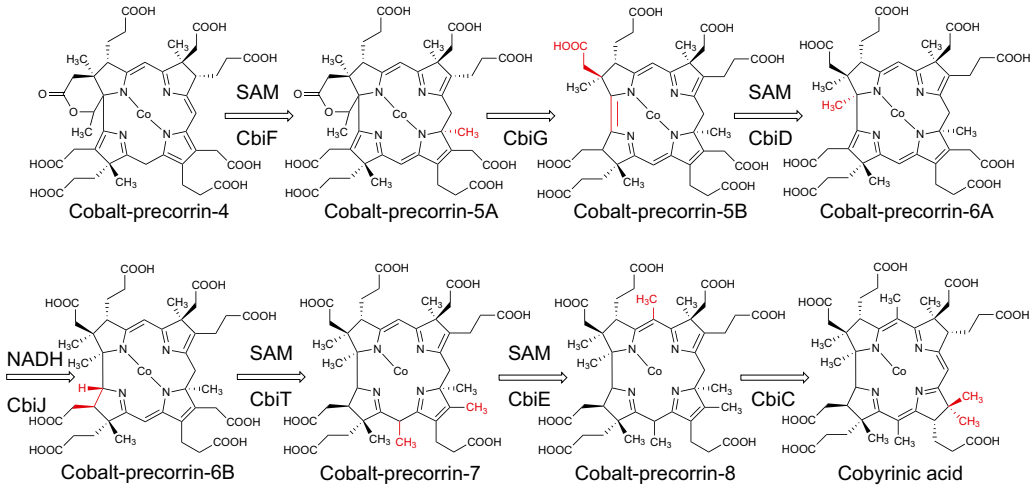

Fig. 4. The anaerobic biosynthesis of cobyrinic acid from cobalt-precorrin-4. The complete step-by-step pathway with enzymes and cofactors is indicated. Cobalt-precorrin-7 was not isolated as part of this study, because the enzymes CbiE and -T are fused into a single protein in *B. megaterium*, allowing the direct conversion of cobalt-precorrin-6B into cobalt-precorrin-8. The tautomeric forms shown are consistent with the EPR and MS data but have not been rigorously confirmed. Indeed, the intermediates may exist as mixtures of tautomers.

biology to assist in the production of new chemicals and drugs through natural synthetic pathways. With the enzymes for corrin ring synthesis now defined for both the aerobic and anaerobic pathways, the potential exists to manipulate the pathway for the construction of vitamin analogs and derivatives.

Materials and Methods

Cloning and Genetic Manipulation. *B. megaterium* DSM509 *cbiF*, *cbiG*, *cbiD*, *cbiJ*, *cbiE*, and *cbiC* were PCR amplified from genomic DNA. The PCR fragment and plasmid were digested with the appropriate restriction enzyme followed by purification, ligation, and transformation of *E. coli* DH10B with 100 μg/mL ampicillin for selection. Table S1 shows plasmids and primers. *B. megaterium* DSM319 was transformed by a modified minimal media protoplast transformation protocol. Full details are in *SI Text*. Enzymes were overproduced and purified as previously described (13) but with modifications (*SI Text*).

Synthesis of Anaerobic Pathway Intermediates. Individual synthesis of intermediates is provided in *SI Text*. As an example, for the enzyme mixture synthesis of cobalt-precorrin-5B, the following protocol is provided. Protein lysates derived from recombinant strains of $CbiH_{60}$ (4 L), CbiF (2 L), and CbiG (0.5 L) were pooled and transferred to the glove box. The pooled lysate was applied to a single immobilized metal affinity chromatography column (7 mL resin) using the standard buffers described. The proteins $CbiH_{60}$, CbiF, and CbiG were purified to homogeneity; 7.5 mL concentrated protein were buffer exchanged into 10.5 mL Buffer H. The incubation contained ~40 mg $CbiH_{60}$, 20 mg CbiF, 15 mg CbiG, 3 mg cobalt-factor III, 21.6 mg SAM, and 43.5 mg sodium dithionite in 10 mL Buffer H. The pH of SAM was adjusted to 8.0 before addition to the reaction. The incubation was left at 37 °C overnight to reach completion (~80% yield) of cobalt-precorrin-5B.

Analytical Analysis. For LC-MS analysis, tetrapyrroles were injected onto an Ace 5 AQ column (2.1 × 150 mm, 5 μm; Advanced Chromatography Technologies) that was attached to an Agilent 1100 series HPLC coupled to a micrOTOF-Q II (Bruker) mass spectrometer equipped with an online diode array run at a flow rate of 0.2 mL min^{-1}. Tetrapyrroles were routinely separated with a linear gradient of acetonitrile in 0.1% (vol/vol) trifluoroacetic acid. For EPR, samples were prepared and then flash-frozen in liquid nitrogen. EPR experiments were performed on a Bruker ELEXSYS E500 Spectrometer operating at X-band using a Super High Q Cylindrical Cavity (Q factor ~ 16,000) equipped with an Oxford Instruments ESR900 Liquid Helium Cryostat linked to an ITC503 Temperature Controller. The experimental parameters are given in the figures. For NMR, all experiments were carried out using a 14.1 T Bruker Avance III Spectrometer (600 MHz ^{1}H resonance frequency) equipped with a QCI (+ ^{19}F) cryoprobe. Resonance assignment was completed using a range of 2D NMR experiments.

ACKNOWLEDGMENTS. We thank Dr. Michelle Rowe and Dr. Karl Fisher for NMR and EPR technical assistance, respectively. This work was supported by British Biotechnology and Biological Sciences Research Council Grants BB/E024203/1 and BB/I012079/1, and Wellcome Trust Equipment Grant 091163/Z/10/Z (to M.J.H. and M.J.W.).

1. Hodgkin DG, et al. (1955) The crystal structure of the hexacarboxylic acid derived from B_{12} and the molecular structure of the vitamin. *Nature* 176(4477):325–328.
2. Blanche F, et al. (1993) Parallels and decisive differences in vitamin B_{12} biosyntheses. *Angew Chem Int Ed Engl* 32(11):1651–1653.
3. Deery E, et al. (2012) An enzyme-trap approach allows isolation of intermediates in cobalamin biosynthesis. *Nat Chem Biol* 8(11):933–940.
4. Debussche L, Thibaut D, Cameron B, Crouzet J, Blanche F (1993) Biosynthesis of the corrin macrocycle of coenzyme B_{12} in *Pseudomonas denitrificans*. *J Bacteriol* 175(22): 7430–7440.
5. Warren MJ, Raux E, Schubert HL, Escalante-Semerena JC (2002) The biosynthesis of adenosylcobalamin (vitamin B_{12}). *Nat Prod Rep* 19(4):390–412.
6. Raux E, Lanois A, Rambach A, Warren MJ, Thermes C (1998) Cobalamin (vitamin B_{12}) biosynthesis: Functional characterization of the *Bacillus megaterium cbi* genes required to convert uroporphyrinogen III into cobyrinic acid *a,c*-diamide. *Biochem J* 335(Pt 1):167–173.
7. Battersby AR (2000) Tetrapyrroles: The pigments of life. *Nat Prod Rep* 17(6):507–526.
8. Uzar HC, Battersby AR, Carpenter TA, Leeper FJ (1987) Biosynthesis of porphyrins and related macrocycles, Part 28. Development of a pulse labelling method to determine the C-methylation sequence for vitamin B_{12}. *J Chem Soc Perkin 1* 1689–1696.
9. Leech HK, et al. (2003) Characterization of the cobaltochelatase $CbiX^{L}$: Evidence for a 4Fe-4S center housed within an MXCXXC motif. *J Biol Chem* 278(43):41900–41907.
10. Brindley AA, Raux E, Leech HK, Schubert HL, Warren MJ (2003) A story of chelatase evolution: Identification and characterization of a small 13-15-kDa "ancestral" cobaltochelatase ($CbiX^{S}$) in the archaea. *J Biol Chem* 278(25):22388–22395.
11. Leech HK, Raux-Deery E, Heathcote P, Warren MJ (2002) Production of cobalamin and sirohaem in *Bacillus megaterium*: An investigation into the role of the branchpoint chelatases sirohydrochlorin ferrochelatase (SirB) and sirohydrochlorin cobalt chelatase (CbiX). *Biochem Soc Trans* 30(4):610–613.
12. Frank S, et al. (2007) Elucidation of substrate specificity in the cobalamin (vitamin B_{12}) biosynthetic methyltransferases. Structure and function of the C20 methyltransferase (CbiL) from *Methanothermobacter thermautotrophicus*. *J Biol Chem* 282(33):23957–23969.
13. Moore SJ, et al. (2013) Characterization of the enzyme $CbiH_{60}$ involved in anaerobic ring contraction of the cobalamin (vitamin B_{12}) biosynthetic pathway. *J Biol Chem* 288(1):297–305.
14. Santander PJ, Roessner CA, Stolowich NJ, Holderman MT, Scott AI (1997) How corrinoids are synthesized without oxygen: Nature's first pathway to vitamin B_{12}. *Chem Biol* 4(9):659–666.
15. Kajiwara Y, Santander PJ, Roessner CA, Pérez LM, Scott AI (2006) Genetically engineered synthesis and structural characterization of cobalt-precorrin 5A and -5B, two new intermediates on the anaerobic pathway to vitamin B_{12}: Definition of the roles of the CbiF and CbiG enzymes. *J Am Chem Soc* 128(30):9971–9978.
16. Wang J, Stolowich NJ, Santander PJ, Park JH, Scott AI (1996) Biosynthesis of vitamin B_{12}: Concerning the identity of the two-carbon fragment eliminated during anaerobic formation of cobyrinic acid. *Proc Natl Acad Sci USA* 93(25):14320–14322.
17. Roessner CA, Williams HJ, Scott AI (2005) Genetically engineered production of 1-desmethylcobyrinic acid, 1-desmethylcobyrinic acid *a,c*-diamide, and cobyrinic acid *a,c*-diamide in *Escherichia coli* implies a role for CbiD in C-1 methylation in the anaerobic pathway to cobalamin. *J Biol Chem* 280(17):16748–16753.
18. Biedendieck R, Yang Y, Deckwer WD, Malten M, Jahn D (2007) Plasmid system for the intracellular production and purification of affinity-tagged proteins in *Bacillus megaterium*. *Biotechnol Bioeng* 96(3):525–537.
19. Spencer P, Stolowich NJ, Sumner LW, Scott AI (1998) Definition of the redox states of cobalt-precorrinoids: Investigation of the substrate and redox specificity of CbiL from *Salmonella typhimurium*. *Biochemistry* 37(42):14917–14927.
20. Nishida Y, Hayashida K, Sumita A, Kida S (1978) Electronic-structures of square-planar cobalt(II), nickel(II) and copper(II) complexes with some N4-macrocyclic ligands.1. *Inorg Chim Acta* 31(1):19–23.
21. Green M, Daniels J, Engelhardt LM (1987) Normal and abnormal electron-spin resonance-spectra of low-spin cobalt(II) [N4]-macrocyclic complexes—a means of breaking the Co-C bond in B_{12} coenzyme. *J Chem Soc Farad T* 1(83):3663–3667.
22. Nishida Y, Hayashida K, Sumita A, Kida S (1980) Electron-Spin Resonance-spectra of square-planar cobalt(II) complexes with various N_4-macrocyclic ligands. *Bull Chem Soc Jpn* 53(1):271–272.
23. Nishida Y, Kida S (1978) Investigation on low-spin cobalt-II complexes. 5. Ground-states of square-planar low-spin cobalt(II) complexes. *Bull Chem Soc Jpn* 51(1):143–149.
24. McGarvey B (1975) Theory of the spin Hamiltonian parameters for low spin cobalt(II) complexes. *Can J Chem* 53(16):2498–2511.
25. Daul C, Schlapfer CW, von Zelewsky A (1979) *The Electronic Structure of Cobalt(II) Complexes with Schiff Bases and Related Ligands. Inorganic Chemistry and Spectroscopy, Structure and Bonding*, eds Clark HJH, et al. (Springer, Berlin), pp 129–171.
26. Trommel JS, Warncke K, Marzilli LG (2001) Assessment of the existence of hyper-long axial Co(II)-N bonds in cobinamide $B(_{12})$ models by using electron paramagnetic resonance spectroscopy. *J Am Chem Soc* 123(14):3358–3366.
27. Bayston JH, Looney FD, Pilbrow JR, Winfield ME (1970) Electron paramagnetic resonance studies of cob(II)alamin and cob(II)inamides. *Biochemistry* 9(10):2164–2172.
28. Chemaly SM, et al. (2011) Probing the nature of the Co(III) ion in corrins: The structural and electronic properties of dicyano- and aquacyanocobyrinic acid heptamethyl ester and a stable yellow dicyano- and aquacyanocobyrinic acid heptamethyl ester. *Inorg Chem* 50(18):8700–8718.
29. Nishida Y, Kida S (1979) Splitting of d-orbitals in square-planar complexes of copper (II), nickel(II) and cobalt(II). *Coord Chem Rev* 27(3):275–298.
30. Raux E, et al. (1996) *Salmonella typhimurium* cobalamin (vitamin B_{12}) biosynthetic genes: Functional studies in *S. typhimurium* and *Escherichia coli*. *J Bacteriol* 178(3): 753–767.
31. Raux E, Lanois A, Warren MJ, Rambach A, Thermes C (1998) Cobalamin (vitamin B_{12}) biosynthesis: Identification and characterization of a *Bacillus megaterium cobI* operon. *Biochem J* 335(Pt 1):159–166.
32. Roessner CA, Scott AI (2006) Fine-tuning our knowledge of the anaerobic route to cobalamin (vitamin B_{12}). *J Bacteriol* 188(21):7331–7334.

Supporting Information

Moore et al. 10.1073/pnas.1308098110

SI Text

Chemicals and Reagents. Most chemicals were purchased from Sigma. Other materials were provided by the following suppliers: restriction and modification enzymes were purchased from Promega and New England Biolabs, molecular biology kits were from Qiagen (QIAprep Miniprep Kit and QIAquick Gel Extraction Kit), chelating-Sepharose fast-flow resin and PD10 columns were from GE Healthcare, tryptone and yeast extract were from Oxoid, and primers were from Fisher Scientific. Sequencing analysis was performed by GATC Biotech.

Minimal Media Protoplast Transformation of *Bacillus megaterium*. A minimal media transformation method was developed for *Bacillus megaterium* DSM319 to improve on the previously published methods (1–3). Prot-Medium (pH 7.5) was composed of the following chemicals dissolved in 1 L water: NH_4Cl (1 g), Tris·HCl (12 g), KCl (35 mg), NaCl (58 mg), $MgSO_4{\cdot}7H_2O$ (267 mg), and $MgCl_2{\cdot}6H_2O$ (4.67 g). Hyp-Medium was prepared aseptically from the following individual autoclaved components: 864 mL Prot-Medium, 136 mL 50% (wt/vol) sucrose, 10 mL 20% (wt/vol) glucose, 6 mL 10% (wt/vol) yeast extract, 2 mL 500 mM KH_2PO_4, and 100 μL 13.25 mM $MnSO_4$. PEG-P solution was composed of 40% (wt/vol) PEG-6000 dissolved in Hyp-Medium (autoclaved at 120 °C for 10 min). For Hyp agar, 1.7% (wt/vol) agar was dissolved in Prot-Medium, autoclaved, and then supplemented with Hyp-Medium components. Hyp top-agar contained 0.9% (wt/vol) agar, which was dissolved in Prot-Medium, autoclaved, and then prepared with Hyp-Medium components.

Protoplast preparation. A preculture of *B. megaterium* DSM319 was grown overnight in 50 mL Hyp-Medium on a shaking platform (100 rpm) at 30 °C for a maximum of 16 h. Hyp-Medium (50 mL) was inoculated with 1 mL preculture, incubated at 37 °C, and shaken at 200 rpm until an OD_{578} of 1.0 was reached (~2 h). Cells were harvested by centrifugation at 2,683 × *g* and 4 °C for 15 min. The supernatant was removed, and cells were resuspended in 5 mL Hyp-Medium. Lysozyme (100 μL 5 mg mL^{-1} dissolved in Hyp-Medium and filter sterilized) was added and incubated at 37 °C with shaking at 100 rpm for 10–20 min until at least 50% of cells were protoplasts (as estimated by use of a light microscope). Protoplasts were incubated on ice for 30 min and then harvested at 1,400 × *g* and 4 °C for 10 min. The supernatant was removed, and cells were resuspended in 5 mL Hyp-Medium. This process was repeated three times to remove excess lysozyme. After the final resuspension in 5 mL Hyp-Medium, 652.5 μL 100% glycerol were added and mixed. Aliquots (500 μL) were prepared and used fresh or stored at −80 °C (viable for 2 mo).

Protoplast transformation. Dried plasmid DNA (~5 μg) was eluted in 50 μL 5 mM Tris·HCl (pH 8) and mixed with 500 μL protoplasts. This solution was added to 1.5 mL PEG-P solution, mixed carefully, and incubated at room temperature for 4 min. Prechilled Hyp-Medium (5 mL) was added and mixed carefully, and protoplasts were harvested by centrifugation (4 min at 1,400 × *g* and 4 °C). The supernatant was discarded carefully, and the pellet was resuspended in 1 mL Hyp-Medium. Protoplasts were regenerated by incubating for 2–3 h at 37 °C with shaking at 100 rpm. Then, protoplast transformation aliquots (100 and 900 μL) were mixed with 7 mL prewarmed Hyp top-agar (42 °C). This mixture was then poured onto prewarmed (37 °C) antibiotic Hyp agar plates, dispersed evenly, and incubated at 37 °C for 24 h. Cells of grown colonies were checked for their rod shape form and streaked again on antibiotic-containing LB agar plates. *B. megaterium* DSM319-derived strains are viable for only 1 wk on a plate at 4 °C. For long-term storage, 20% (vol/vol) glycerol stocks were prepared at −80 °C.

Overproduction and Purification of *B. megaterium* Cobalamin Enzymes. After protoplast transformation of *B. megaterium* DSM319, recombinant strains were grown in 0.1–4 L LB containing 10 μg mL^{-1} tetracycline at 25–30 °C. On reaching an OD_{578} of 0.3, protein production was induced with 0.25% (wt/vol) xylose and left to grow overnight at 25–30 °C. Cells were collected by centrifugation (5,180 × *g* at 4 °C for 15 min) and resuspended in 15 mL binding buffer (20 mM Tris·HCl, pH 8, 500 mM NaCl, 5 mM imidazole). Cells were lysed by sonication followed by centrifugation at 37,044 × *g* at 4 °C for 20 min. The purification of $CbiH_{60}$ was carried out in an anaerobic glove box (Belle Technology), whereas the rest of the proteins were purified aerobically. Recombinant proteins were purified using immobilized metal affinity chromatography as previously described. A summary of protein purification and yields is provided in Table S2.

Protocol for the Synthesis of the Anaerobic Vitamin B_{12} Pathway Intermediates. All enzyme incubations were conducted under anaerobic conditions in an anaerobic glove box (<2 ppm). Enzymes were exchanged into Buffer H (50 mM Tris·HCl, pH 8.0, and 400 mM NaCl), and enzyme concentrations were estimated by absorbance at 280 nm. Either DTT or dithionite was used as an artificial electron source for the factor to precorrin reductase activity of $CbiH_{60}$.

Cobalt(II)-precorrin-4. This synthesis was achieved by incubating 20 mg $CbiH_{60}$, 3 mg cobalt(II)-factor III, 10.8 mg *S*-adenosyl-L-methionine (SAM), and 43.5 mg sodium dithionite in a total volume of 10 mL buffer H. The reaction was incubated at 37 °C in the dark until completion (~24 h).

Cobalt(II)-precorrin-5A. This synthesis was achieved by incubating 20 mg CbiF, 2 mg cobalt(II)-precorrin-4, 4.3 mg SAM, and 15.4 mg DTT in a total volume of 10 mL buffer H. DTT was added to prevent the oxidation of cobalt(II)-precorrin-4 to cobalt-factor IV. The reaction was incubated at 37 °C in the dark until completion (~2–4 h).

Cobalt(II)-precorrin-5B. This synthesis was achieved by incubating 5 mg CbiG and 1 mg cobalt(II)-precorrin-5A in a total volume of 10 mL buffer H. The reaction was incubated at 37 °C in the dark until completion (~30 min). Alternatively, a direct synthesis from cobalt(II)-factor III could be achieved for large-scale synthesis (EPR and NMR sample preparations) as described in *Materials and Methods*.

Cobalt(II)-precorrin-6A. This synthesis was achieved by incubating 5 mg CbiD, 5 mg cobalt(II)-precorrin-5B, and 4.3 mg SAM in a total volume of 10 mL buffer H. The reaction was incubated at 30 °C in the dark until completion (~6–10 h).

Cobalt(II)-precorrin-6B. This synthesis was achieved by incubating 1 mg CbiJ, 5 mg cobalt(II)-precorrin-6A, and 7.4 mg NADH in a total volume of 10 mL buffer H. The reaction was incubated at 25 °C until completion (~1–2 min).

Cobalt(II)-precorrin-8. This synthesis was achieved by incubating 10 mg CbiET, 2.5 mg cobalt(II)-precorrin-6B, and 8.6 mg SAM in a total volume of 10 mL buffer H. The reaction was incubated at 37 °C until completion (~1–2 h).

Cob(II)yrinic acid. This synthesis was achieved by incubating 4 mg CbiC and 2.5 mg cobalt(II)-precorrin-8 in a total volume of 10 mL buffer H. The reaction was incubated at 37 °C until completion (~6–10 h).

Purification of Anaerobic Pathway Intermediates. Reactions were stopped by heating the incubations to 70 °C for 30 min. They were centrifuged at 39,191 × *g* for 15 min in anaerobic centrifuge tubes to remove precipitate. To remove residual His_6-tagged enzymes, the supernatant was passed through a nickel-chelated Sepharose column and washed with 20 mM Tris·HCl (pH 8) and 200 mM NaCl. The flow-through fractions were pooled together and then diluted in ddH_2O, and therefore, the NaCl concentration was less than 50 mM. Intermediates were then bound to an anion-exchange DEAE–Sepharose (Sigma) column and washed sequentially with 20 mM Tris·HCl (pH 8) containing 100, 200, and 500 mM NaCl. Intermediates eluted between 200 and 500 mM NaCl. For additional purification (except cobalt-precorrin-6A and -6B), the pH was adjusted to 4.0 with 1 M acetic acid before applying to a LiChroprep RP18 column equilibrated with water (adjusted to pH 4.0). The pigment was then briefly washed with water and 10% ethanol and eluted in 50% ethanol. After lyophilisation, intermediates were resuspended in water or (for LC-MS analysis), 1% (vol/vol) acetic acid.

Estimation of the Extinction Coefficient of Cobalt-Precorrin-6A. To estimate the concentration of cobalt-precorrin-6A, NADH (0–50 μM) was gradually titrated into a reaction containing cobalt-precorrin-6A (A_{335nm} = 1.12) and 1 μM CbiJ at 25 °C. After each addition of NADH (1 μM), the reaction was left until completion (<1 min) before rescanning. During the titration, isosbestic points at 329, 407, and 426 nm remained constant, whereas the blue shift from 436 to 419 nm was monitored (Fig. S4*C*). Saturation of this spectral shift occurred at 22 μM NADH. This observation provided an indication of the substrate concentration, with the extinction coefficient of cobalt-precorrin-6A estimated at ε_{335nm} = 50,900 M^{-1} cm^{-1}.

NMR Sample Preparation. The sample for NMR analysis of dicyanocob(III)yrinic acid was prepared by multienzyme synthesis using purified *B. megaterium* enzymes and cofactors. After the incubation, the mixture containing the intermediate was heated to 75 °C for 30 min to precipitate some of the enzymes, which were subsequently removed by centrifugation (2,683 × *g* for 10 min). The supernatant was then bound to a DEAE column and washed with 20 mM potassium phosphate buffer (pH 8) with an increasing concentration of NaCl (100 and 200 mM NaCl). The tetrapyrrole was eluted with 20 mM potassium phosphate buffer (pH 8) containing 600 mM NaCl. This fraction was passed through an immobilized metal ion affinity column and washed through with 20 mM potassium phosphate buffer (pH 8) containing 200 mM NaCl to remove residual His_6-tagged proteins. Fractions were pooled, and 10 mM KCN was added and left overnight. The pH was subsequently adjusted to 4.0 with 1 M acetic acid before applying to a LiChroprep RP18 column equilibrated with water (adjusted to pH 4.0). The pigment was briefly washed with water and 10% ethanol and eluted in 50% ethanol. The sample was transferred into a Wilmad screw-cap 5-mm NMR tube. All NMR experiments were carried out using a 14.1 T Bruker Avance III Spectrometer (600 MHz ^1H resonance frequency) equipped with a QCI (+ ^{19}F) cryoprobe. Resonance assignment was completed using a range of 2D NMR experiments, including ^{13}C-^1H heteronuclear single quantum coherence (HSQC) and heteronuclear multiple bond correlation (HMBC) as well as ^1H-^1H homonuclear correlation, rotating frame Overhauser effect (ROESY), and total correlation (TOCSY) NMR experiments. All 2D datasets were recorded with 4,096 and 1,024 points in the direct and indirect dimensions, respectively. ^{13}C-^1H HSQC datasets were recorded using ^1H and ^{13}C spectral widths of 9,615 and 25,652 Hz, respectively; ^{13}C-^1H HMBC datasets were recorded using ^1H and ^{13}C spectral widths of 7,211 and 33,474 Hz, respectively. All ^1H-^1H correlation datasets were recorded with direct and indirect dimension spectral widths of 7,211 and 7,200 Hz, respectively.

Instability of Cobalt-Precorrin-6A and -6B for NMR. Cobalt-precorrin-6A and -6B could not be distinguished by LC-MS because of its sensitivity to acidification, a requirement for HPLC purification. Several samples of cobalt-precorrin-6A and -6B were prepared by the same method used for the purification of cobalt-precorrin-8 and cobyrinic acid. However, despite only two major peaks detected on LC-MS (951 and 949 Da), a complex mixture was observed by NMR, representing several tautomeric forms (Fig. S7*A*). Because of the discrepancies observed by MS and NMR for cobalt-precorrin-6A and -6B, acidification was thought to be the cause of these problems. To avoid this problem, 5 mg cobalt-precorrin-6B were purified in alkaline buffer (5 mM potassium phosphate buffer, pH 8) by anion-exchange chromatography and eluted in 0.6 M NaCl. The sample was filtered by centrifugation (2,683 × *g* for 1 h) through an Amicon 10,000 MWCO Concentrator to remove protein contaminants. The filtrate was dried and resuspended in 300 μL D_2O with an approximate concentration of 5 M NaCl. We attempted to measure a low-resolution ^1H ^{13}C HSQC using a 3-mm NMR tube to increase sensitivity at this high-salt concentration. From this spectrum, we could detect approximately five methyl groups (Fig. S7*B*), which likely correspond to the C-1, C-2, C-7, C-11, and C-17 methyl positions. Despite this result, the quality of the spectra was too low to continue with additional experiments (ROESY, TOCSY, HMBC, and ^1H-^1H homonuclear correlation) and assignments. In conclusion, cobalt-precorrin-6A and -6B are both remarkably sensitive to acid and too unstable to analyze by NMR.

1. Barg H, Malten M, Jahn M, Jahn D (2005) Protein and vitamin production in *Bacillus megaterium*. *Microbial Processes and Products*, ed Barredo JL (Humana Press, Totowa, NJ), Vol. 18, pp 165–184.
2. Fodor K, Hadlaczky G, Alföldi L (1975) Reversion of Bacillus megaterium protoplasts to the bacillary form. *J Bacteriol* 121(1):390–391.
3. Meinhardt F, Stahl U, Ebeling W (1989) Highly efficient expression of homologous and heterologous genes in Bacillus megaterium. *Appl Microbiol Biotechnol* 30(4):343–350.

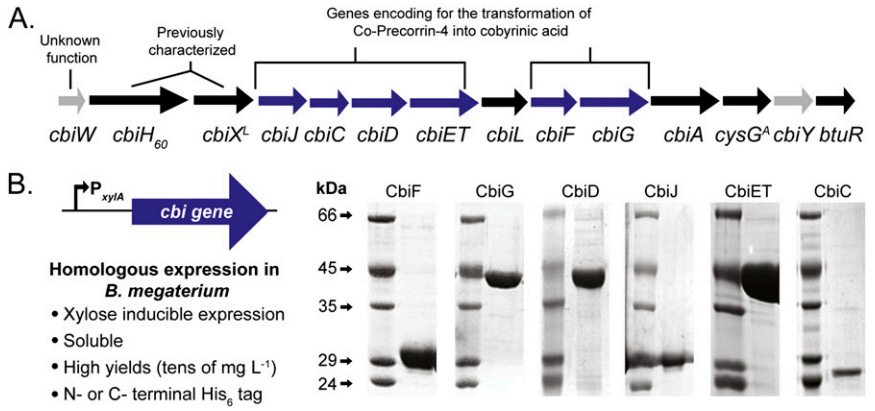

Fig. S1. Homologous protein expression in *B. megaterium* DSM319 of anaerobic pathway enzymes. (*A*) *B. megaterium* DSM509 *cobI* operon. (*B*) Summary of the expression system and SDS/PAGE of purified enzymes. A basic characterization and approximate yields of the recombinant proteins are provided in Table S2.

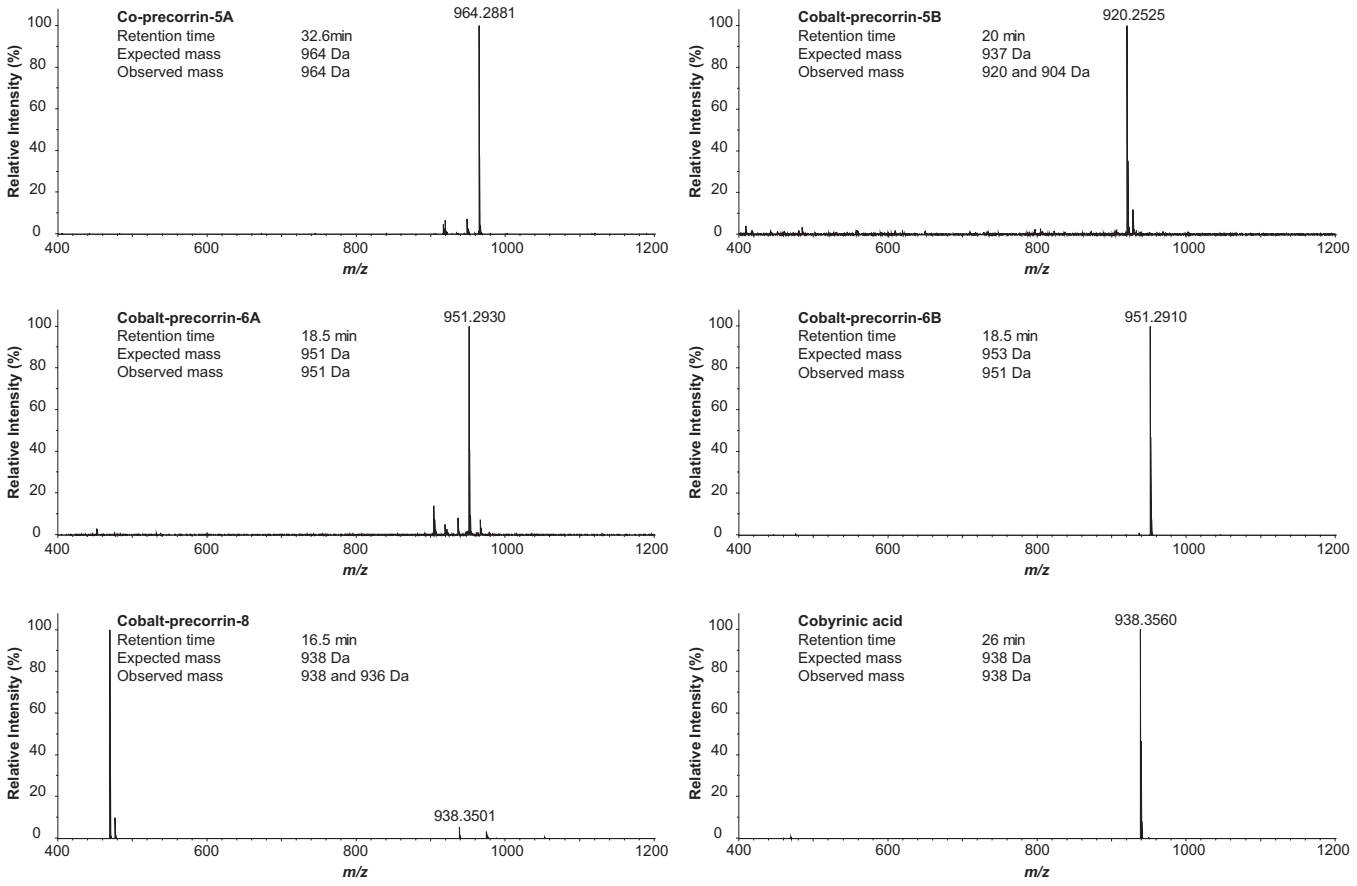

Fig. S2. Mass spectra of anaerobic pathway intermediates. All intermediates were synthesized anaerobically step by step from cobalt-precorrin-4 (*m/z* 950) using purified CbiF, CbiG, CbiD, CbiJ, CbiET, and CbiC. Samples were separated by reverse-phase LC using a linear gradient of 5–100% acetonitrile in 0.1% trifluoroacetic acid.

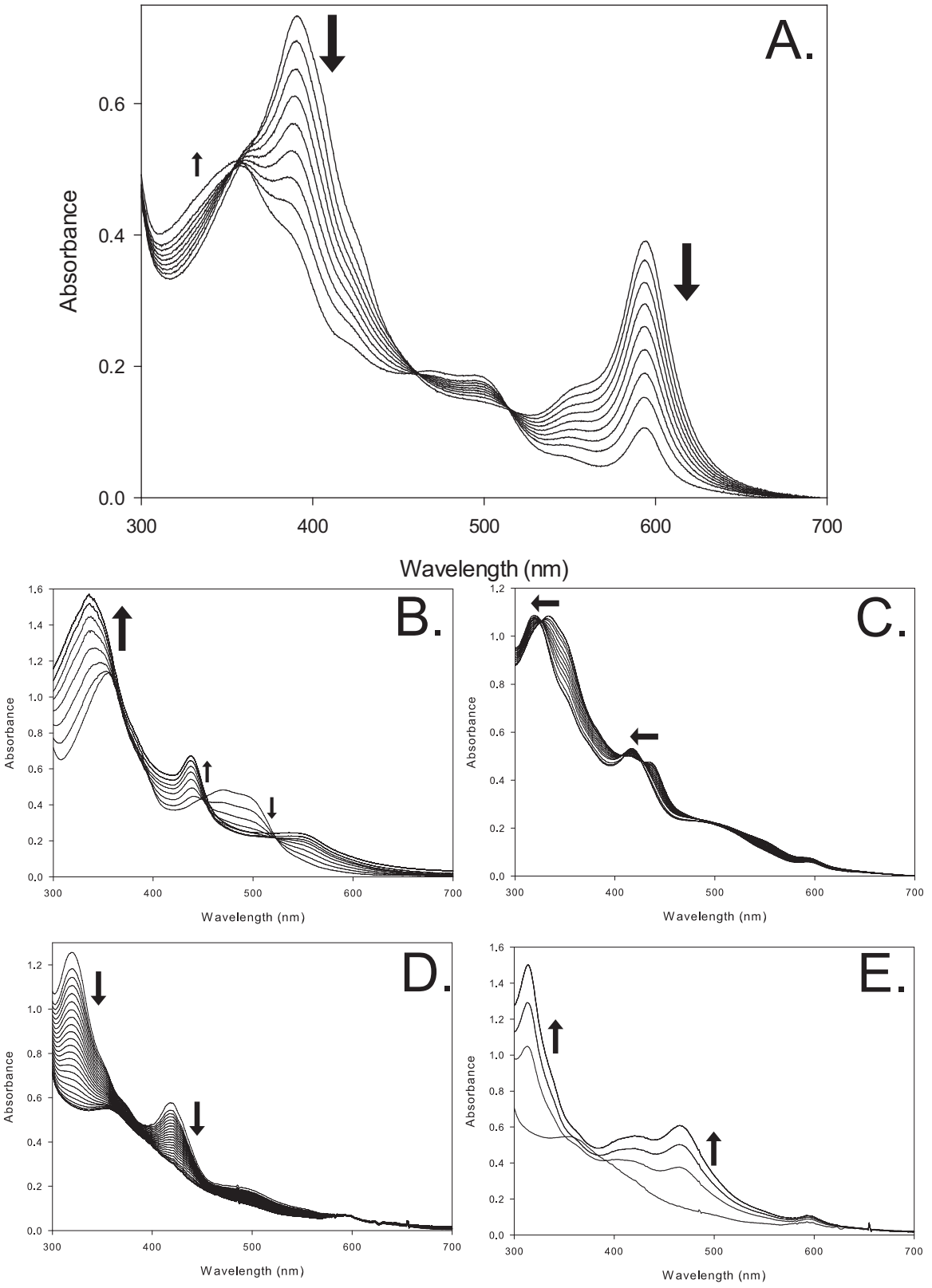

Fig. S3. UV-Vis spectra of the anaerobic pathway reactions. (*A*) Synthesis of cobalt-precorrin-5B from cobalt-factor III by the enzymes $CbiH_{60}$, CbiF, and CbiG. (*B*) Synthesis of cobalt-precorrin-6A by CbiD. (*C*) Synthesis of cobalt-precorrin-6B by CbiJ. (*D*) Synthesis of cobalt-precorrin-8 by CbiET. (*E*) Synthesis of cobyrinic acid by CbiC.

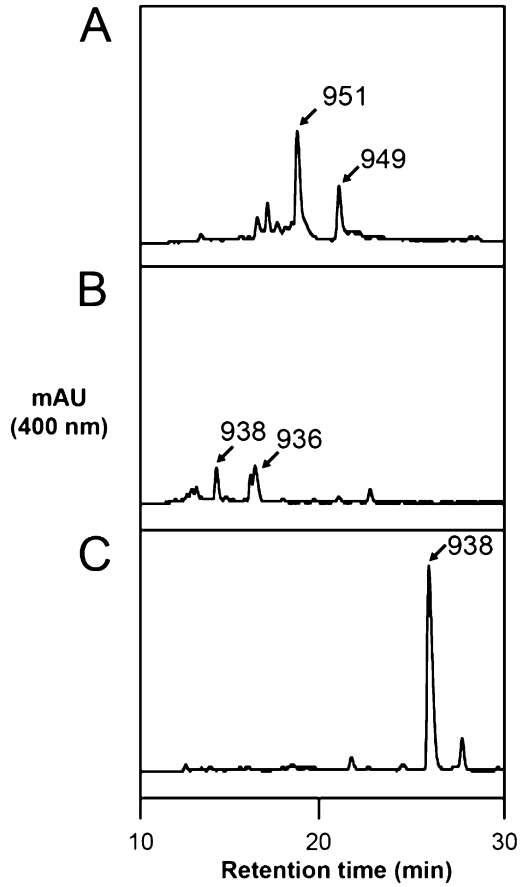

Fig. S4. LC-MS of anaerobic pathway intermediates. Mass spectra are shown in Fig. S1. (*A*) Cobalt-precorrin-6B is detected at 951 and 949 Da, which are two and four units less than its expected mass of 953 Da. (*B*) Cobalt-precorrin-8 is detected at its correct mass (938 Da) and 936 Da. (*C*) Cobyrinic acid is detected as a single peak at 938 Da. Note that a number of degradation peaks are observed with cobalt-precorrin-6B and cobalt-precorrin-8, whereas cobyrinic acid elutes as a single peak (~90%) and is the only intermediate that we could determine its structure by NMR.

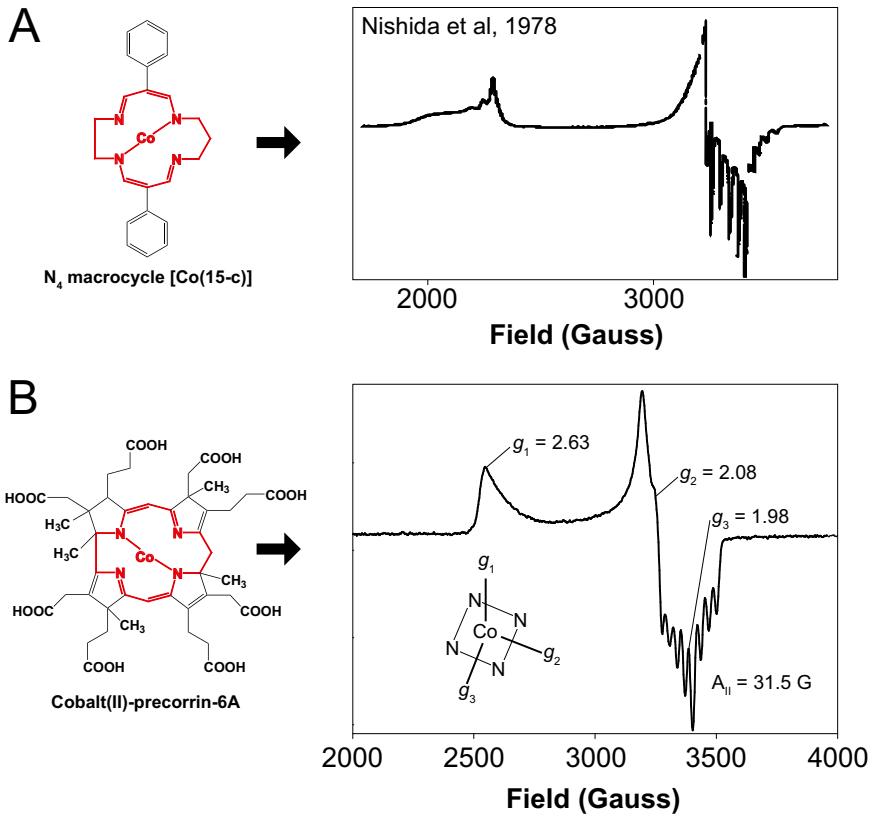

Fig. S5. EPR spectra of the d_{yz} cobalt(II) coordination state. (*A*) Structure and EPR spectra of Co-N_4 macrocyle. Modified from Nishida et al. (1). (*B*) Structure and EPR spectra of cobalt(II)-precorrin-6A.

1. Nishida Y, Hayashida K, Sumita A, Kida S (1978) Electronic-structures of square-planar cobalt(II), nickel(II) and copper(II) complexes with some N_4-macrocyclic ligands. *Inorg Chim Acta* 31:19–23.

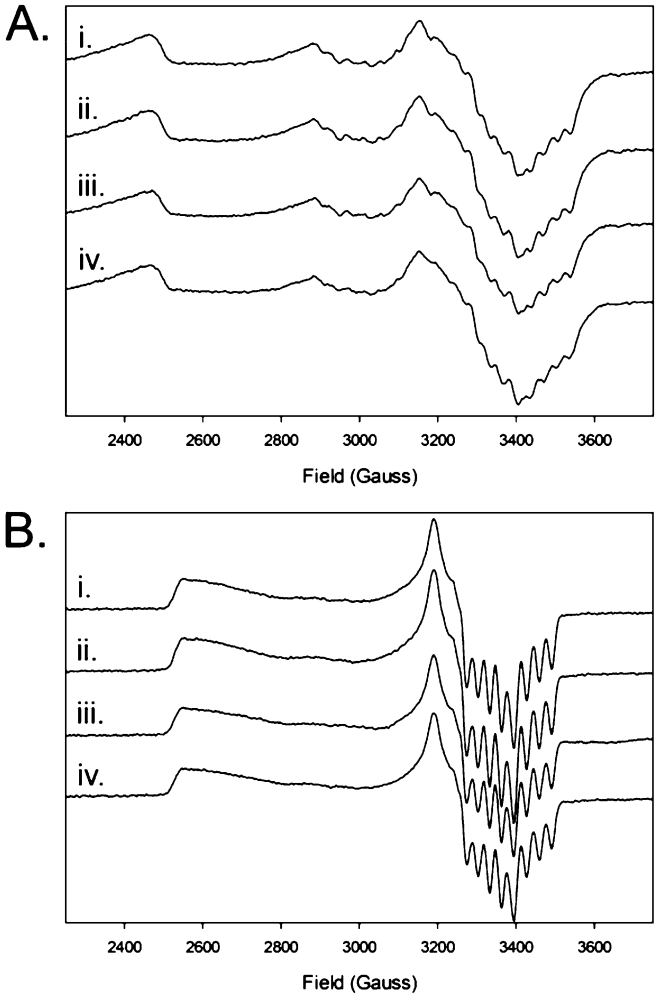

Fig. S6. Negative control EPR spectra of methyltransferase reactions: (*A*) 200 μM cobalt(II)-precorrin-5B (*i*) on its own, (*ii*) with 1 mM SAM, (*iii*) with 50 μM CbiD after initial mixing, and (*iv*) with 50 μM CbiD after 24 h incubation at 30 °C; (*B*) 200 μM cobalt(II)-precorrin-6B (*i*) on its own, (*ii*) with 1 mM SAM, (*iii*) with 50 μM CbiET after initial mixing, and (*iv*) with 50 μM CbiET after 24 h incubation at 37 °C.

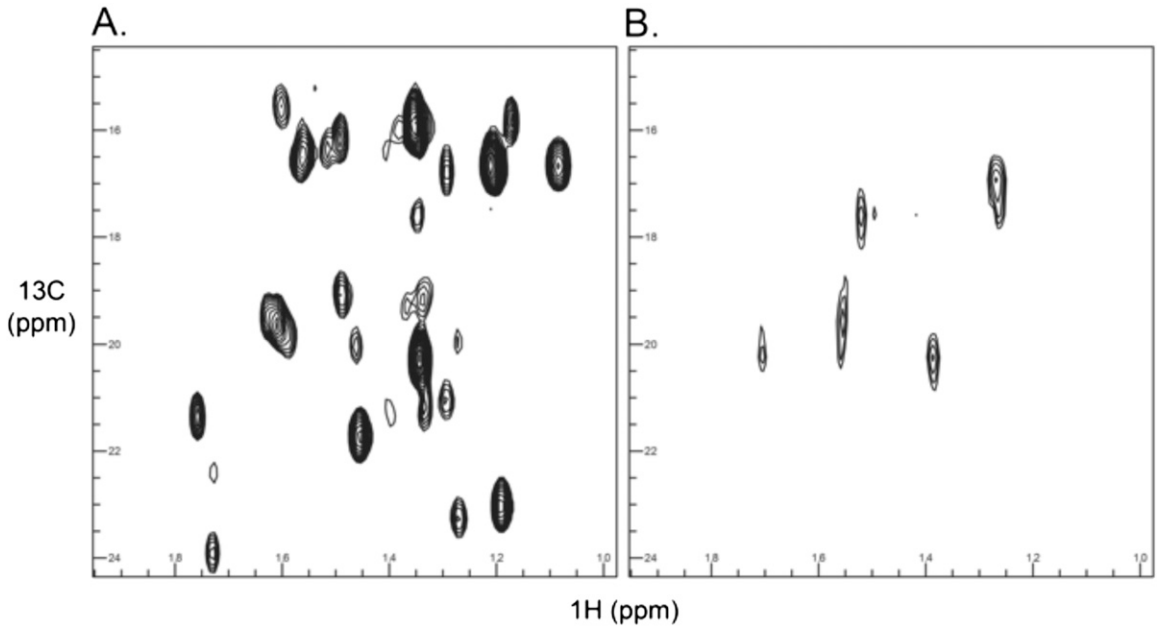

Fig. S7. ^{1}H ^{13}C HSQC of methyl group region in cobalt-precorrin-6B: (*A*) 5-mg sample prepared by standard purification (DEAE and RP-18) in D_2O (5-mm tube); (*B*) 5-mg sample purified (DEAE only) with 5 M NaCl in D_2O (3-mm tube).

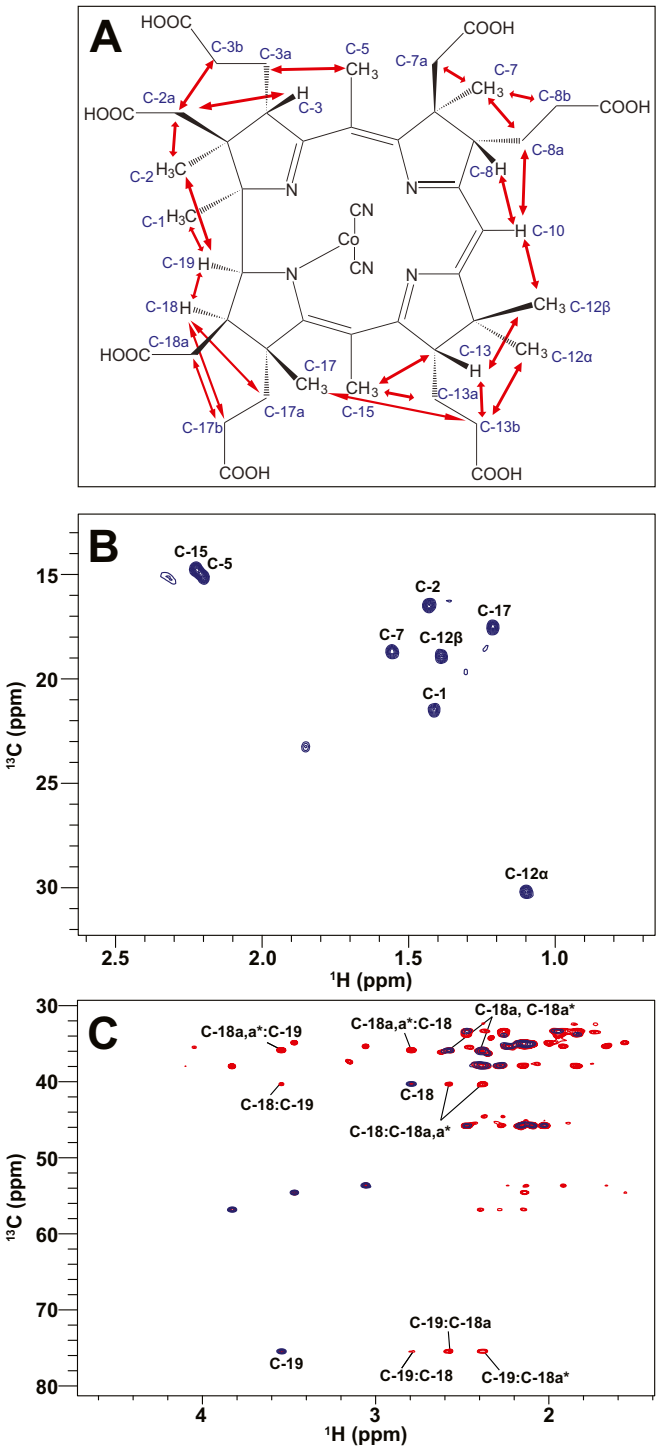

Fig. S8. 2D NMR of in vitro-synthesized cobyrinic acid (3 mM). (*A*) Structure of dicyanocobyrinic acid with ^{1}H-^{13}C points labeled in blue. Through-space nuclear Overhauser effect contacts observed in the ROESY spectrum are shown as red arrows. (*B*) ^{1}H-^{13}C HSQC of methyl group region with methyl group positions labeled. (*C*) Region showing the ^{1}H-^{13}C HSQC (blue) and ^{1}H-^{13}C HSQC-TOCSY (red) connections between the C-18a, C-18a* (*prochiral), C-18, and C-19 positions. The C-18/C-19 position is sp^3 and provides indirect evidence of the reduction catalyzed by CbiJ earlier in the pathway.

Table S1. Plasmids and primers

Name	Description	Source
pAR8766	16.3 kb *B. megaterium cobI operon* (Sau3AI fragment) cloned into BamHI site of pKK223.3	1
pETcoco-2-*ABCDCXL*	Expression in *Escherichia coli* of His_6-tagged proteins for multienzyme synthesis of cobalt-factor III	2
pC-His1622	Derivative of pWH1520 for intracellular production of C-terminal His_6-tagged proteins in *B. megaterium*	3
pN-His-TEV1622	Derivative of pWH1520 for intracellular production of N-terminal His_6-tagged proteins in *B. megaterium*	3
pSJM73	*B. megaterium cbiG* PCR cloned into pC-His1622 with BglII and SphI	This work
pSJM78	*B. megaterium cbiJ* PCR cloned into pC-His1622 with BglII and SphI	This work
pSJM116	*B. megaterium cbiF* PCR cloned into pC-His1622 with BsrGI and BamHI	This work
pSJM188	*B. megaterium* $cbiH_{60}$ as previously described	2
pSJM195	*B. megaterium cbiD* PCR cloned into pC-His1622 with BglII and SphI	This work
pSJM231	*B. megaterium cbiC* PCR cloned into pN-His-TEV1622 with BglII and EagI	This work
pSJM236	*B. megaterium cbiET* PCR cloned into pC-His1622 with BglII and SphI	This work
Primer	Sequence	Restriction enzyme
cbiF Forward	GCGTGTACAATGAAGTTATACATAATCGGAGCTGG	XbaI
cbiF Reverse	CATGGATCCTTTCCGATTTCACTCC	BamHI
cbiG Forward	CACAGATCTGGATGATTCAACTCGAAGAAG	BglII
cbiG Reverse	CATGCATGCTTGTCATATGGAATAAGTGC	SphI
cbiD Forward	CACAGATCTGGATGAAGGAAGTCGCAAAAGAACC	BglII
cbiD Reverse	GTGGCATGCTTATTGCCATGTTGCACC	SphI
cbiJ Forward	CACAGATCTGGATGATTTTATTGTTAGCTGG	BglII
cbiJ Reverse	CATGCATGCTTACTCCTGGTTTGG	SphI
cbiET Forward	CACAGATCTGGATGGCAATTAAAATTATTGG	BglII
cbiET Reverse	GTGGCATGCTTTTCTCCTCTTTTGGCTG	SphI
cbiC Forward	CATAGATCTGGATGGATTTTCGTACAG	BglII
cbiC Reverse	GTGCGGCCGGGTTCTTTTGGCACTTCCTTC	EagI

1. Raux E, Lanois A, Warren MJ, Rambach A, Thermes C (1998) Cobalamin (vitamin B_{12}) biosynthesis: Identification and characterization of a *Bacillus megaterium* cobI operon. *Biochem J* 335(Pt 1):159–166.
2. Moore SJ, et al. (2013) Characterization of the enzyme $CbiH_{60}$ involved in anaerobic ring contraction of the cobalamin (vitamin B_{12}) biosynthetic pathway. *J Biol Chem* 288(1):297–305.
3. Biedendieck R, Yang Y, Deckwer WD, Malten M, Jahn D (2007) Plasmid system for the intracellular production and purification of affinity-tagged proteins in *Bacillus megaterium*. *Biotechnol Bioeng* 96(3):525–537.

Table S2. Expression, yield, and buffer stabilization of *B. megaterium* DSM509 cobalamin enzymes

Enzyme	Temperature (°C)	Yield (mg/L)	Molecular mass (kDa)	p*I*	Oligomeric state (FPLC)	Stable buffer at 5 mg/mL	
						Buffer (20 mM)	Salt
$CbiX^{L}$*	37	20–30	36.0	5.9	Dimer	Tris·HCl	100 mM NaCl
$CbiL^{\dagger}$	28	0–1	31.7	8.3	Dimer	Tris·HCl	100 mM NaCl
$CbiH_{60}$	28	10–30	64.7	5.9	Dimer	Tris·HCl	400 mM NaCl
CbiF	28	10–30	32.4	8.8	Dimer	Tris·HCl	400 mM NaCl
CbiG	21	50–100	45.4	6.0	Dimer	KPi, pH 8.0	—
CbiD	28	5–10	43.3	7.2	Monomer	Hepes, pH 7.5	100 mM NaCl
CbiJ	28	20–30	31.6	8.4	Dimer	Na-citrate, pH 5.5	—
CbiET	28	10–30	48.3	5.8	Tetramer	Hepes, pH 7.5	—
CbiC	28	1–5	29.3	6.5	Dimer	Tris·HCl, pH 8	100 mM NaCl
$CbiW^{\ddagger}$	28	10–20	18.7	8.3	ND	Tris·HCl, pH 8	100 mM NaCl

*As described by Leech et al. (1).
†Low expression and difficult to reproduce.
‡Insoluble and purified by denaturing and refolding from inclusion bodies.

1. Leech HK, et al. (2003) Characterization of the cobaltochelatase $CbiX^{L}$: Evidence for a 4Fe-4S center housed within an MXCXXC motif. *J Biol Chem* 278(43):41900–41907.

Table S3. EPR *g* values and hyperfine coupling constants

Intermediate	$g_\perp$	$g_\parallel$		$A_\parallel$ (G)
d_z2 intermediates				
Cobalt-factor III	2.28	2.002		113
Cobalt-factor IV	2.28	1.993		144
Cobalt-precorrin-4	2.25	2.002		113
Cobalt-precorrin-8	2.24	2.006		87
Cobyrinic acid	2.23	2.000		110
	g_1	g_2	g_3	A_3 (G)
d_{yz} intermediates				
Cobalt-precorrin-5A	2.65	2.06	1.97	32.8
Cobalt-precorrin-5B	2.72	2.06	1.96	31.8
Cobalt-precorrin-6A	2.63	2.08	1.98	31.5
Cobalt-precorrin-6B	2.63	2.08	1.98	30.3

Table S4. NMR chemical shift assignments for dicyanocobyrinic acid in D_2O

Number	Group	δ^1H (ppm)	δ^{13}C (ppm)
C-3	CH	3.83	56.84
C-8	CH	3.47	54.58
C-10	CH	5.76	91.08
C-13	CH	3.06	53.64
C-18	CH	2.79	40.28
C-19	CH	3.54	75.43
C-2a	CH_2	2.15	45.72
C-3a	CH_2	2.17, 2.13	25.97
C-3b	CH_2	2.39, 2.28	37.83
C-7a	CH_2	2.47, 2.03	45.75
C-8a	CH_2	2.17, 2.10	35.01
C-8b	CH_2	2.00, 1.56	27.70
C-13a	CH_2	1.91, 1.67	27.39
C-13b	CH_2	2.23, 2.12	35.35
C-17a	CH_2	1.85	33.73
C-17b	CH_2	2.26	33.94
C-18a	CH_2	2.59, 2.38	36.00
C-1	CH_3	1.41	21.51
C-2	CH_3	1.43	16.49
C-5	CH_3	2.20	15.07
C-7	CH_3	1.56	18.71
C-12α	CH_3	1.10	30.20
C-12β	CH_3	1.39	18.93
C-15	CH_3	2.23	14.78
C-17	CH_3	1.21	17.52